Hindawi
Security and Communication Networks
Volume 2022, Article ID 9851533, 12 pages
https://doi.org/10.1155/2022/9851533

Research Article

Nonlinear Lamb Wave for Structural Incipient Defect Detection with Sequential Probabilistic Ratio Test

Hanxin Chen ,[1,2] Mingming Liu,[2] Yongting Chen,[3] Shaoyi Li,[1] and Yuzhuo Miao[2]

[1]*School of Artificial Intelligence, Nanchang Institute of Science and Technology, Nanchang 330108, Jiangxi, China*
[2]*School of Mechanical and Electrical Engineering, Wuhan Institute of Technology, Wuhan 430074, Hubei, China*
[3]*Wuhan Britain-China School, Wuhan 430035, Hubei, China*

Correspondence should be addressed to Hanxin Chen; pg01074075@ntu.edu.sg

Received 10 January 2022; Revised 26 January 2022; Accepted 14 February 2022; Published 9 March 2022

Academic Editor: Muhammad Arif

The incipient defect is difficult to be identified by ultrasonic signal analysis. The nonlinear ultrasonic method based on the nonlinear Lamb wave principle is proposed by establishing a nonlinear Lamb wave ultrasonic inspection platform. The optimal Lamb wave parameters are obtained for the incipient fatigue material defects. The aluminum alloy board with 3 mm thickness under the different fatigue tensile cycles is tested. The nonlinear ultrasonic signals are analyzed to obtain second harmonic signals. The intelligent diagnosis method for incipient material degrade is proposed based on the Sequential Probability Ratio Test (SPRT). The sequential probabilistic ratio test (SPRT) algorithm is carried out to classify and identify the second harmonics of four different fatigue damages. The results show that the method about with nonlinear Lamb wave analysis with SPRT is effective and reliable for the incipient material microdefect degradation.

1. Introduction

With the rapid development of the intelligent industry, the quick requirement for the quality control of the large scale mechanical system in the industrial areas of the transportation, energy, and chemical production is increased. It is a great challenge for the nondestructive testing techniques such as ultrasonic methods to regularly maintain the reliability of the key equipment structures under the premise of considering the operation cost. Currently, the typical NDT that is widely used includes X-ray, magnetic powder, and eddy current that are not economical and reliable due to the long detection cycle, small detection range, and high cost. The ultrasonic detection technology has the advantages, which results in the common applications in the fault diagnosis of the mechanical structural system. The principle of ultrasonic detection technology is that the ultrasonic signal is excited to propagate into the mechanical structural material to produce interface reflection or cause sound speed and energy attenuation after encountering defects [1].

The research shows that the nonlinear ultrasonic testing technology overcomes the limits and deficiency of the traditional ultrasonic nondestructive testing, which is effective to detect the early damage of mechanical structural materials. Especially, the traditional linear Lamb wave detection technology is poor for the microdefect of the mechanical structural material identification, which inspired the nonlinear ultrasonic detection technology to be starting applications in the mechanical industry [2, 3]. Therefore, the nonlinear Lamb wave detection technology [4–6] is introduced in the detection of the fatigue degradation of the mechanical structural material.

Lamb wave is used as a guide wave, which has the superiority and advantages in the NDT applications such as little attenuation, lasting test distance, and fast spread [7]. It is a hot research topic discussing the fundamental nonlinear ultrasonic theory and applications for the diagnosis of the microdefects in alloy sheet structures. The limit and deficiency of the nonlinear Lamb wave are that propagation of Lamb wave in the plate is characteristic of the dispersion phenomenon and various modes, which make the signal processing complex. It is key point to select the optimal modes of Lamb wave to make full use of the optimal ultrasonic physical mechanism for mechanical structural material detection. The large number of the theoretical analysis and experiments has been done for the nonlinear ultrasonic testing. Wang et al. studied the second harmonic generation of the nonlinear ultrasonic Lamb waves and analyzed the feasibility of Lamb wave to detect the defects in the board [8]. Bermes et al. used the nonlinear Lamb wave to detect the fatigue damage of materials that the material property change was much sensitive to the second harmonic wave and the nonlinear coefficients, which has become larger when the propagation distance increased [9, 10]. Pruell [11] et al. studied the implementation of the second harmonic of nonlinear Lamb waves. The observation characteristics in the frequency domain distinguish the fatigue cracks. Martin [12] et al. proposed the method to detect the material nonlinearity by utilizing nonlinear Lamb wave, which shows that Lamb wave has great potential in the applications of the nondestructive evaluation of the thin plate structure. The nonlinear effect of Lamb wave was generated for the 6061-T6 and 1100-H14 aluminum alloy test materials.

Wald [13] proposed a new hypothesis testing method—sequential probabilistic ratio test in 1947. Goodman et al. [14] adopted a method based on the combination of the adaptive waveform and sequential probability ratio test to identify radar signals. Min et al. [15] summarized the sequential probabilistic ratio test algorithms based on parameters and nonparameters. Chen et al. used the sequential probability ratio test algorithm to analyze and study the fault modes of gearbox [16] and proposed a method for multiple fault identification of gearbox based on the sequential probability ratio test.

In this paper, sequential probabilistic ratio test algorithm is proposed to classify the second harmonic signals extracted from nonlinear Lamb wave detection. The nonlinear Lamb wave detection system is established. According to the dispersion curve, four 2A12 aluminum alloy plates with different fatigue degrees were detected by selecting suitable modal Lamb waves, and the second harmonic signals were collected. The kurtosis value is extracted by time domain analysis method for sequential probabilistic ratio test, and the collected second harmonic signals with different fatigue degrees are classified effectively.

2. Lamb Wave Mechanism and Signal Analysis

2.1. The Fundamental Theory about Lamb Wave. Lamb wave is generated as the stress wave as shown in Figure 1. The two conditions for Lamb wave are necessary when the ultrasonic signal propagates in a thin metal plate: the thickness of the thin plate is equivalent to the wavelength of the Lamb wave. It is subjected to alternating surface tension and the particle produces the horizontal and vertical vibration. The vibration synthesizes the elliptical trajectory vibration. This elliptical trajectory is the propagation process of Lamb waves.

Lamb wave detection has the following advantages: the received signal includes the information of the whole detection area; Lamb wave detects many defects in difficult contact positions; Lamb wave has the advantages of the long propagation distance, small attenuation, and high efficiency. The common applications in the detection methods are mechanical impedance, wave propagation detection, and phased array.

Based on the characteristics of the vibration displacement of the ultrasonic particle, the propagation mode of the Lamb wave is classified as the symmetric mode and the antisymmetric mode as shown in Figure 2. Symmetric modes are denoted as $S0, S1, S2, S3, \ldots$. The symmetry mode is characterized by the longitudinal vibration of the center particle and elliptical motion of the upper and lower surface particles that have the opposite phases and are symmetric by the center. The antisymmetric mode is denoted as $A0, A1, A2, A3, \ldots$. The antisymmetric mode consists of the transverse vibration of the center particle and elliptical motion of the upper and lower surface particles, which has the same phase with the asymmetry for the center.

The precondition for separating the symmetric mode and antisymmetric mode of Lamb wave is that only the ultrasonic signal propagating along the symmetry axis of the plate is decomposed into the symmetric mode and antisymmetric mode. The Rayleigh-Lamb frequency equation for the symmetric mode and antisymmetric mode is described as the wave-motion characteristics of Lamb.

Symmetric model [17] is defined as

$$\begin{cases} \Phi = A_2 \cos(px_3) \\ \Psi = B_1 \sin(qx_3) \\ u = ikA_2 \cos(px_3) + qB_1 \sin(qx_3) \\ v = -pA_2 \cos(px_3) - ikB_1 \sin(qx_3) \\ \sigma_{31} = \mu\left[-2ikpA_2 \sin(px_3) + \left(k^2 - q^2\right)B_1 \sin(qx_3)\right] \\ \sigma_{33} = -\lambda\left(k^2 + q^2\right)A_2 \cos(px_3) - 2\mu\left[p^2 A_2 \cos(px_3) + ikqB_1 \cos(qx_3)\right] \end{cases} . \quad (1)$$

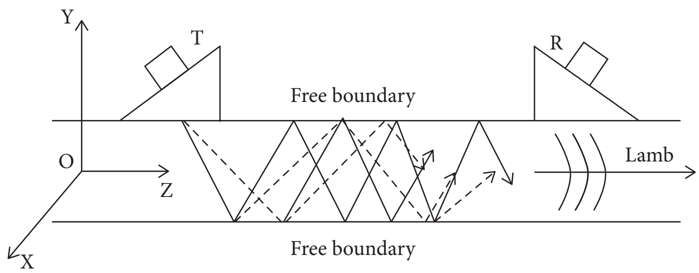

Figure 1: Lamb wave propagation.

Antisymmetric model is described as

$$\begin{cases} \Phi = A_2 \cos(px_3) \\ \Psi = B_2 \sin(qx_3) \\ u = ikA_1 \cos(px_3) + qB_2 \sin(qx_3) \\ v = -pA_1 \cos(px_3) - ikB_2 \cos(qx_3) \\ \sigma_{31} = \mu\left[2ikpA_1 \cos(px_3) + \left(k^2 - q^2\right)B_2 \cos(qx_3)\right] \\ \sigma_{33} = -\lambda\left(k^2 + p^2\right)A_1 \sin(px_3) - 2\mu\left[p^2 A_1 \sin(px_3) + ikqB_2 \sin(qx_3)\right] \end{cases}. \tag{2}$$

Here, the parameters μ and λ are Lamb wave constants, and the parameters Φ and Ψ are the compressional and shear waves that functions as control. The parameters u and v represent displacement fields, the parameters σ_{31} and σ_{33} represent stress fields, and the variables p and q are set parameters. The unknown constants A_1, A_2, B_1, B_2 are determined by the zero-stress boundary conditions. The parameters $\sigma_{31} = \sigma_{33}$ are described by the geometrical problem of the free plate. By further simplifying (1) and (2), the symmetric modes and antisymmetric modes of Lamb waves are obtained as follows:

Symmetric model:

$$\frac{\tan(qb)}{\tan(pb)} = -\frac{4k^2 pq}{\left(q^2 - k^2\right)^2}. \tag{3}$$

Antisymmetric model:

$$\frac{\tan(qb)}{\tan(pb)} = -\frac{\left(q^2 - k^2\right)^2}{4k^2 pq}. \tag{4}$$

The parameters p and q in the above equation are obtained from $p^2 = \omega^2/c_l^2 - k^2$ and $q^2 = \omega^2/c_t^2 - k^2$. The parameter $\omega = 2\pi\lambda/c_p$ is the angular frequency, the parameter c_p is the phase velocity of the Lamb wave, the parameter c_l is the p-wave velocity, the parameter c_t is the s-wave velocity, and the parameter b is 1/2 the thickness of the plate. The dispersion curve is generated from the relationship between phase velocity c_p and angular frequency ω as defined in (3) and (4). The longitudinal wave velocity and transverse wave velocity are defined in (5) and (6).

$$c_l = \sqrt{\frac{E(1-v)}{\rho(1+v)(1-2v)}}, \tag{5}$$

$$c_t = \sqrt{\frac{E}{2\rho(1+v)}}. \tag{6}$$

Here, the parameter E is the elastic modulus of the material, the parameter ρ is the material density, and the parameter v is the Poisson's ratio. The relation between phase velocity c_p and group velocity c_g is shown in

$$c_g = d\psi/d\left(\psi/c_p\right). \tag{7}$$

In formula (7), the parameter ψ is the angular velocity. The longitudinal wave velocity $c_l = 6441m/s$ and transverse wave velocity $c_t = 3224m/s$ were measured for the aluminum alloy plates. The phase rate and group rate dispersion curves of Lamb wave in aluminum alloy board are obtained by solving the Rayleigh-Lamb equation with MATLAB numerical method as shown in Figure 3.

It is shown that the dispersion curve of Lamb wave has the following characteristics: except for modes $A0$ and $S0$, all other modes have cutoff frequency phenomenon. There are at least two modes of the waveform at each frequency that has different phase velocity and group velocity. The dispersion occurs in all modes. As shown in the dispersion curves of phase velocity and group velocity, the dispersion and multimodal phenomena exist simultaneously during the propagation of Lamb. At least three modes appear when the frequency density matches the condition as defined in $f \cdot d \geq 3MHz \cdot mm$. When the frequency density meets the condition as defined in $f \cdot d \leq 2.5MHz \cdot mm$, only two

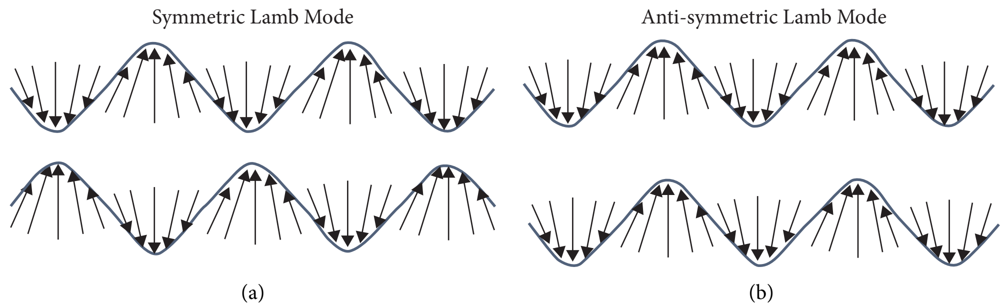

Figure 2: Symmetric mode (a) and antisymmetric mode (b) of Lamb wave.

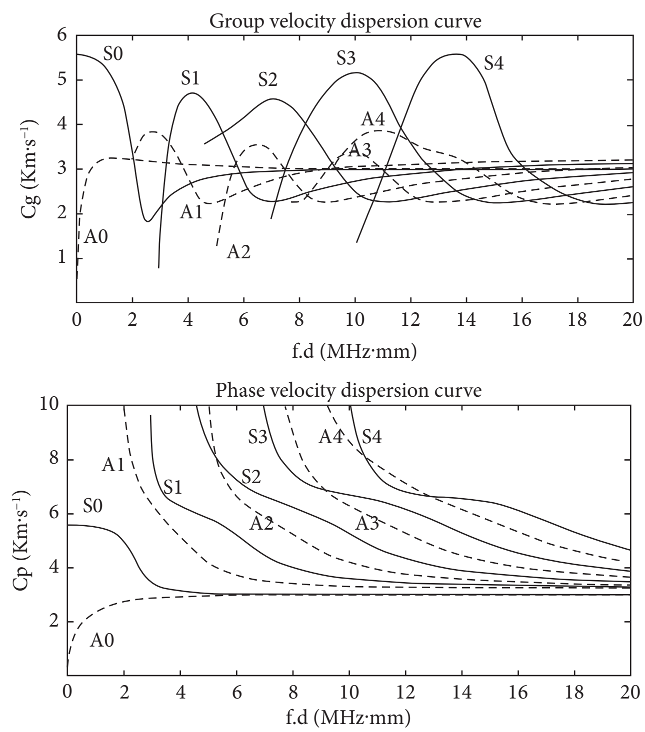

Figure 3: Phase velocity dispersion curve and group velocity dispersion curve.

modes A0 and S0 exist, which is used to select the center frequency of the excitation signal.

When Lamb waves with the specific modes is used to generate the nonlinear ultrasonic signals, Snell's law as defined in $\theta = \sin^{-1}(C_w/C_p)$ is used to define the excitation angle curve of Lamb waves in aluminum alloy sheet as shown in Figure 4. The parameter θ is the excitation angle. The parameter C_w is the longitudinal wave velocity of the transducer. The parameter C_p is the magnitude of the phase velocity. When the frequency density $f \cdot d$ and emission angle θ are determined, Lamb waves of specific modes are excited. It is shown in Figure 4 that the incident angle of Lamb wave excited by $S0$ mode is 50°. Because of the influence of the manufacture technique of the transducer and the material properties of the specimen, the actual incident angle fluctuates around 50°.

The use of nonlinear ultrasound to characterize early defects (microplastic deformation, microcracks, holes, and features such as residual stresses) in mechanical components is the use of ultrasound nonlinear characteristic parameters to characterize the material nonlinear properties of metallic components, which is the domain of the inverse problem of fatigue damage analysis of metals. The material nonlinear properties of metallic components are expressed based on the intrinsic structure relationship (i.e., stress-strain relationship) of the solid material. There is a quantitative relationship between the nonlinear coefficients in the solid material intrinsic structure relationship and the elastic constants of the structure. When stress or fatigue damage exists within a metallic material, the second-order elastic constant values do not change much, but the third-order elastic constant values change significantly. Since the third-order elastic constants are more sensitive to fatigue characteristics such as microplastic deformation, microcracks, or residual stresses in metallic materials, the nonlinear ultrasonic detection characteristic parameters have a higher sensitivity to fatigue characteristics such as microplastic deformation, microcracks, or residual stresses than the linear ultrasonic characteristic parameters (such as sound velocity and sound attenuation).

2.2. Sequential Probabilistic Ratio Test. The fundamental concept of the sequential probabilistic ratio evaluation is as follows: the data x is observed to get $x_1, x_2, x_3, \ldots\ldots x_n$ as a series of unconstrained evenly distributed random variables. The parameters $x_1, x_2, x_3, \ldots\ldots x_n$ represent n random variables. Two hypotheses are proposed for the samples: null hypothesis H_0: $\theta = \theta_0$ and alternative hypothesis H_1: $\theta = \theta_1$, which constitute a binary sequential probabilistic ratio test. The joint probability density is defined as shown in in

$$f_j(x) = p\left(x_1, \ldots, x_n \mid H_j\right) = \prod_{i=1}^{n} f\left(x_i/\theta_j\right). \tag{8}$$

Here, the variable $j = 0, 1$. The likelihood ratio λ_n of the sequential probabilistic ratio test is calculated by

$$\lambda_n(x) = \lambda_n(x_1, \ldots, x_n) = \frac{p(x_1, \ldots, x_n \mid H_1)}{p(x_1, \ldots, x_n \mid H_0)} = \frac{\prod_{i=1}^{n} f(x_i/\theta_1)}{\prod_{i=1}^{n} f(x_i/\theta_0)}. \tag{9}$$

Here, the function $f(x/\theta)$ is the conditional probability distribution and the variable θ is the distribution parameter. The thresholds A and B (where $A > B$) are determined

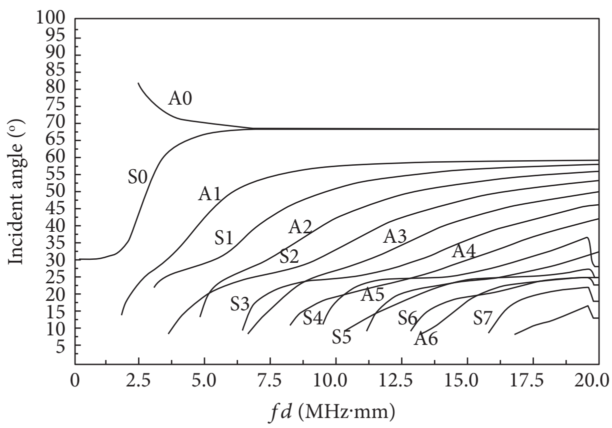

Figure 4: Excitation angle curve.

according to the probability α of type in the first error and the probability β of type in the second error in the hypothesis test, which is defined in

$$A = \frac{1-\beta}{\alpha}, \tag{10}$$

$$B = \frac{\beta}{1-\alpha}. \tag{11}$$

The data x_1 is assumed as the first value. The likelihood ratio $\lambda_1(x_1)$ is calculated by formula (9), which is compared with the set thresholds A and B to identify the two fatigue damage modes. The likelihood ratio $\lambda_1(x_1)$ satisfies the following inequality:

$$\lambda_1(x_1) < B. \tag{12}$$

Then, the test is stopped, the null hypothesis H_0 is accepted, and the alternative hypothesis H_1 is rejected. The likelihood ratio satisfies

$$\lambda_1(x_1) > A. \tag{13}$$

Thus, the test is stop, the alternative hypothesis H_1 is accepted, and the null hypothesis H_0 is rejected. The likelihood ratio meets the following inequality:

$$B \leq \lambda_1(x_1) \leq A. \tag{14}$$

Then, the next set of values is selected for testing. The above steps are repeated until the requirements for stopping testing are met. The final judgment is given. Figure 5 shows the flow chart of the sequential probabilistic ratio test.

3. Nonlinear Lamb Wave Experiment

3.1. Nonlinear Lamb Wave Detection System. The nonlinear detection system is shown in Figure 6. The experimental system consists of the RAM-5000-SNAP platform, computer, 50 Ω impedance, attenuator, filter, and amplifier. The experimental nonlinear ultrasonic system is designed by using the different modules as shown in Figure 7. The parameters in the nonlinear system are optimized for incipient defect detection. The RAM-5000-SNAP has great advantages in exciting the large amplitude ultrasonic wave and accurately receiving and identifying the second harmonic wave that is reflected by the material defects. The nonlinear system is connected to the computer. The parameters of the experimental instruments are controlled by the computer software. A single mode transmitter is used for the incident signal and two receivers collected the experimental data. The excited ultrasonic signal generated by RAM-5000-SNAP is generated from the excitation probe, transmitted to the material specimen, the impedance, the low-pass filter, and the receiving probe. When the ultrasonic signal of Lamb wave propagates in the aluminum alloy plate to meet the microcrack, the waveform distortion is presented. The second harmonic and the higher harmonics are generated. The higher harmonics above the second harmonic are characteristic of the weak changes and easily sheltered by the system noise from the nonlinear ultrasonic platform. The second harmonics are mainly considered as the identification features and parameter. The receiving channel (End 1) of the RAM-5000-SNAP collects the original signals without any preprocessing. The receiving channel (end 2) receives the second harmonic signals preprocessed by the high-pass wave filter and semaphore amplifier. The oscilloscope displays and collects the test signal to present the nonlinear ultrasonic signals online.

The 2.5MHz sinusoidal pulse series was selected as the excitation signal center frequency. The experimental nonlinear Lamb detection platform is designed to detect the microdefects of aluminum alloy sheet, which required the ipsilateral excitation receiving method for the excitation probe and receiving probe to be adopted that is suitable for sheet structure detection. The excitation probe and receiving probe are located on the same side of the specimen. Hanning window is used to optimize the excitation signal, because the sinusoidal pulse signal modulated by Hanning window has more concentrated energy that is compared with the general sine wave signal. The energy dissipation of the excited guided wave signal in the propagation process is smaller, which reduces the attenuation of ultrasonic wave and the scattering of waves, which makes the ultrasonic guided wave easier to propagate in the specimen. The nonlinear effect of the received signal is much better. Figure 8(a) shows the time domain diagram and frequency domain diagram of the signal modulated by Hanning window. Figure 8(b) shows the time domain and frequency domain of the signal that is not modulated by Hanning window. It is presented in the frequency domain signal that the peak values of the fundamental wave and the sidelobes of other frequencies beside the fundamental wave exist. The energy of the original signal is dispersed to other frequencies, which is not beneficial to the detection of the nonlinear ultrasound. The Hanning window modulation method is used to suppress the influence of the transient process on the original Lamb wave.

The optimal number of the excitation cycles is tested and selected. No dispersion at the same frequency and more cycles in a single pulse make the frequency domain of the received signal narrower and the signal clearer. As it is proved that the more cycles there are, the narrower the frequency-domain signal bandwidth is and the purer the

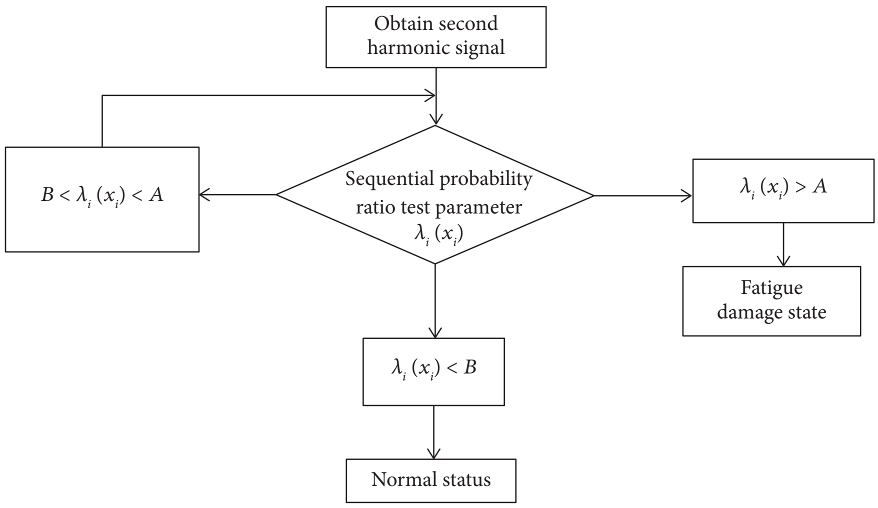

FIGURE 5: Flow chart of sequential probabilistic ratio test.

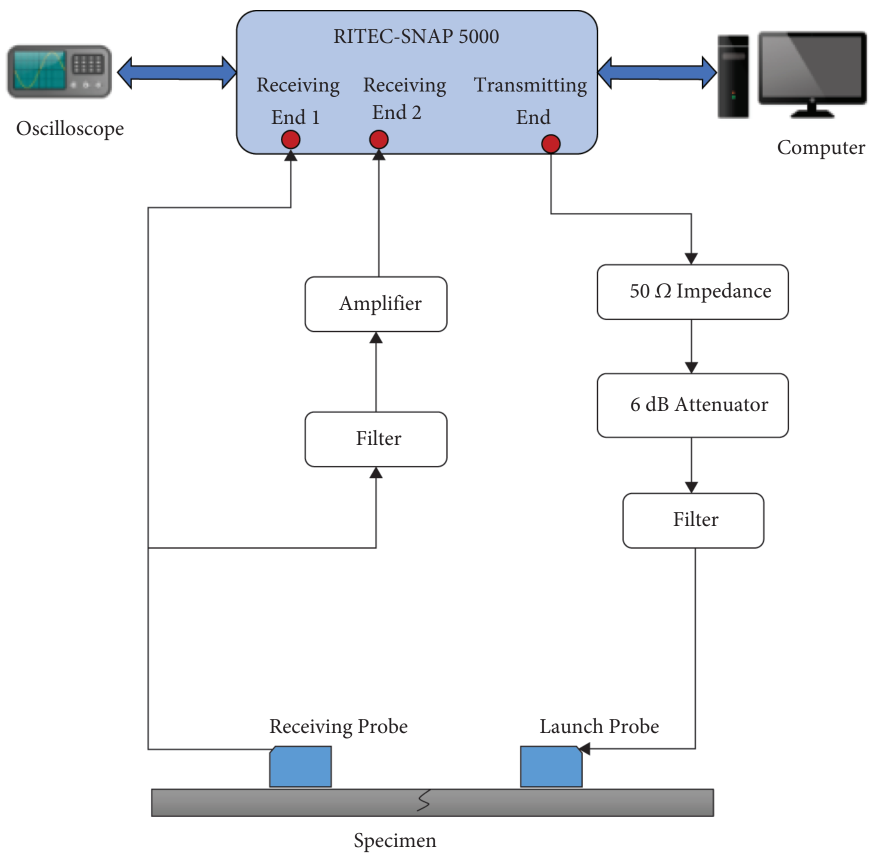

FIGURE 6: Nonlinear ultrasonic system.

signal is causing the energy to exceed the instrument range without changing the energy of the single cycle excitation signal. The disadvantage of many cycles is that the amplitudes of the time-domain need to be reduced accordingly. It is necessary for the time-domain detection to set the optimal cycles. The 15 cycles were selected for the nonlinear Lamb detection experiment. It is considered for the good contact between the probe and the surface of the specimen during the experiment. The couplant needs to be contacted evenly to minimize the error to make the experimental signals accurate.

3.2. Specimens. The sample pieces in the experiment are 2A12 aluminum alloy plate, as shown in Figure 9. The size is $300 \times 100 \times 3$ (mm^3). The density is $\rho = 2800kg/m^3$. The modulus of elasticity is $E = 72.4GPa$ and Poisson's ratio is $v = 0.33$. The main components of 2A12 aluminum alloy are shown in Table 1. A triangular notch is cut on the top of the sheets that are labeled as 1, 2, 3, 4, respectively, to induce the fatigue. Then cycles of the fatigue stretches were 0, 4000, 8000, and 12000, which is performed on the four plates. The schematic of the specimen structure is shown in Figure 8. For the second harmonic signals obtained in the experiment, fatigue stretching signals are recorded as normal signals S1, and 4,000, 8,000, and 12,000 fatigue damage signals are recorded as $S2$, $S3$, and $S4$, respectively.

4. Sequential Probability Ratio Test for Nonlinear Lamb Wave Analysis

4.1. Feature Extraction of Nonlinear Lamb Wave. The characteristic information of the ultrasonic signals collected in the experiment is reflected by the characteristic parameters. The experimental nonlinear Lamb waves are processed by noise reduction filtering. The characteristic parameters are extracted from the collected second harmonic signals. The characteristic parameters are used as the test data for the sequential test. Because kurtosis value is sensitive to the fatigue damage signal of the aluminum alloy plate, which is used as characteristic parameters in this paper. Suppose $x_i = [x_1, x_2, x_3, \ldots, x_N]$ is a list of randomly distributed data to be tested, $N = 2000$. The 1901 testing points are taken for each group. The 100 groups of test data are obtained. The calculation formula of characteristic parameters is as follows:

$$\begin{aligned} \overline{x} &= \frac{1}{N}\sum_{i=1}^{N} x_i, \\ k &= \frac{1901 \times \sum_{i=t}^{t+1900} (x_i - \overline{x})^4}{\left(\sum_{i=t}^{t+1900} (x_i - \overline{x})^2\right)^2}, \quad t = 1, 2, 3, \ldots, 100. \end{aligned} \tag{15}$$

The extracted kurtosis values are the sequence to be examined $k_i = [k_1, k_2, k_3, \ldots, k_n]$. The mean and standard deviation of the kurtosis values are defined as follows:

$$\begin{aligned} \mu &= \frac{1}{n}\sum_{i=1}^{n} k_i, \\ \sigma &= \sqrt{\frac{1}{n}\sum_{i=1}^{n}\left(k_i - \overline{k}\right)^2}. \end{aligned} \tag{16}$$

4.2. Algorithm for SPRT. The likelihood ratio formula is such that both mean value and standard deviation have great influence on the likelihood ratio. The testing sequences satisfy the Gaussian distribution roughly. When there is no crack in the aluminum alloy specimen, the collected second harmonic signal sequence satisfies the null hypothesis H_0: $\theta = \theta_0$ and when there is fatigue crack, the signal sequence satisfies the alternative hypothesis H_1: $\theta = \theta_1$. During the test, the standard deviation σ remains the same, only the mean value changes. Under the condition that both the null hypothesis and the alternative hypothesis are true, the joint probability density of the signal sequence is expressed as

$$P_{ji}(k_i) = \frac{1}{\sigma\sqrt{2\pi}} \exp\left[-\frac{1}{2\sigma^2}\left(k_i - \mu_j\right)^2\right]. \tag{17}$$

Here, when $j = 0$, $P_{0i}(k_i)$ represents the probability density function of the null hypothesis and $j = 1$, $P_{1i}(k_i)$ represents the probability density function of the alternative hypothesis, the likelihood ratio of sequential probability ratio test is obtained as follows:

$$\lambda_i = \frac{\prod_{i=0}^{n} P_{1i}(k_i)}{\prod_{i=0}^{n} P_{0i}(k_i)} = \frac{P_{11}(k_1)P_{12}(k_2)\cdots P_{1i}(k_i)}{P_{01}(k_1)P_{02}(k_2)\cdots P_{0i}(k_i)} \times \frac{P_1}{P_0}. \tag{18}$$

The parameter P_1 is the transcendental probability under the alternative hypothesis when $i = 0$. The parameter P_0 is the prior probability of the null hypothesis when $i = 0$. For the sake of simplifying the calculation and facilitate applications, (18) above is converted into the following form [13]:

$$\Delta = \mathrm{In}\,\lambda_i = \mathrm{In}\frac{\prod_{i=0}^{n} P_{1i}(k_i)}{\prod_{i=0}^{n} P_{0i}(k_i)} = \sum_{i=0}^{n} \mathrm{In}\frac{P_{1i}(k_i)}{P_{0i}(k_i)}. \tag{19}$$

At this point, the threshold $a = \mathrm{In}A$ and $b = \mathrm{In}B$. According to the sequential probability ratio theory mentioned in Section 1, when the likelihood ratio satisfies $\Delta < b$, sampling is stopped and H_0 is accepted, which is the normal state. When $\Delta > a$, stop sampling and accept H_1, that is, the fatigue damage state. If $b < \Delta < a$, it cannot be determined at this time, and then sampling shall be continued and compared with a and b with the next likelihood ratio, until the above conditions are met and the sampling is stopped and the judgment is made.

5. Results and Discussion

The second harmonic signal is the main characteristic signal which characterizes the nonlinear effect. The second harmonic signal is extracted and analyzed to identify the fatigue degradation. The four groups of the second harmonic signals are obtained by the experimental setup, which label $S1$ in normal state and $S2$, $S3$, and $S4$ in three fatigue damage states as shown in Figure 10. The label $S1$ is the second harmonic signal collected by specimens without fatigue damage. The samples $S2$, $S3$, and $S4$ are the second harmonic signals, which is collected from the fatigue materials with 4000, 8000, and 12,000 cycles.

It is shown from the likelihood ratio formula of the sequential probability ratio test that the likelihood ratio is highly dependent on the variation of the mean values. The mean values of $S1$ in the nonfatigue state is set as the parameter μ_0. The average values of $S2$, $S3$, and $S4$ in the fatigue damage state are set as μ_1 to test and classify the signals. The test results are shown in Figure 11.

The average value of the second harmonic semaphore $S1$ in the undamaged state is taken as the variable μ_0. The average value of the second harmonic signal $S2$ in the fatigue damage state is taken as the variable μ_1. In Figure 11(a), the

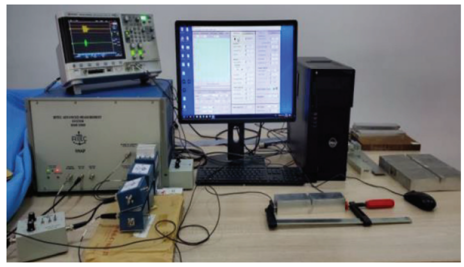

Figure 7: Experimental platform setup of nonlinear Lamb detection.

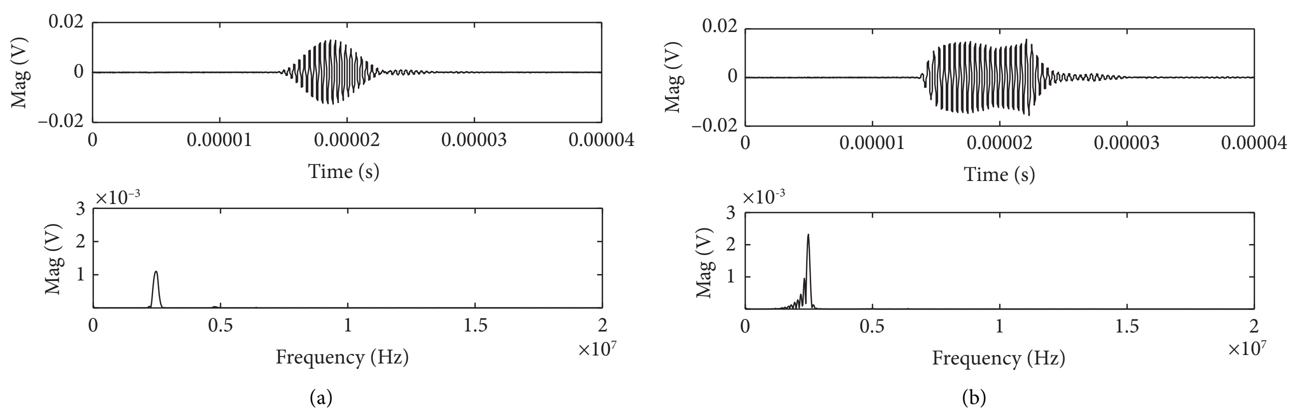

Figure 8: (a) Signal representation with Hanning window modulation. (b) Signal representation without Hanning window modulation.

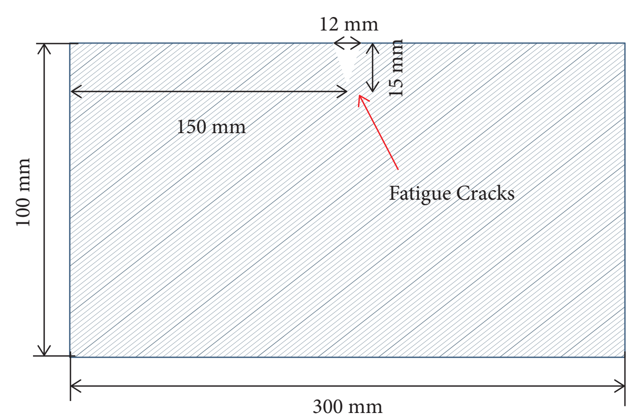

Figure 9: The sample with introduced crack.

Table 1: Main components of 2A12 aluminum alloy.

Chemical composition	Cu	Si	Fe	Mn	Mg	Zn	Cr	Ti	Al
Scale scores	3.8–4.9	0.5	0.5	0.3–0.9	1.2–1.8	0.3	—	0.15	Remaining

ten nonlinear Lamb ultrasonic signals under $S1$ and $S2$ samples are obtained and input into the likelihood ratio formula. The likelihood ratio meets $\Delta < b$ and the aluminum alloy specimen is judged to be normal state without fatigue damage, when the likelihood ratio meets $\Delta > a$ and the fatigue damage state of the aluminum alloy specimen with 4000 cycles fatigue damage is judged. In Figure 11(b), the mean values of $S1$ in the undamaged state and $S3$ in the fatigue damage state are taken as parameters μ_0 and μ_1 for testing, respectively. The test SPRT are obtained as shown in Figure 11(b). When the experimental ultrasonic signal S1 is input, the likelihood ratio meets $\Delta < b$, which indicates that the aluminum alloy specimen has no fatigue damage. When the signal $S3$ is inputted, the likelihood ratio meets $\Delta > a$, which indicates that the aluminum alloy specimen has fatigue damage with 8000 fatigue cycles. In Figure 11(c), the

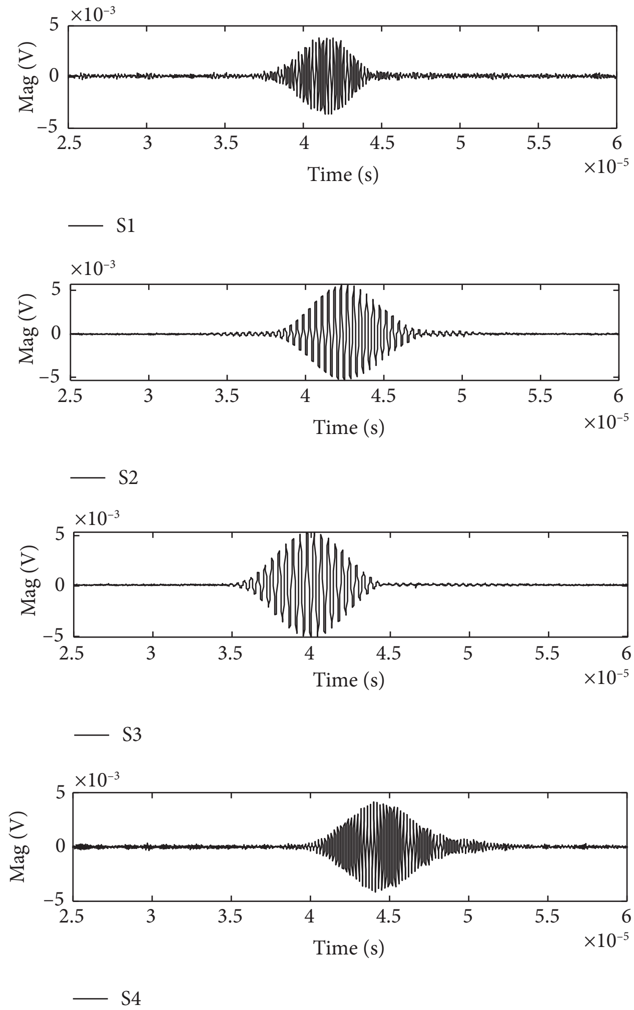

Figure 10: Four sets of second harmonic signals.

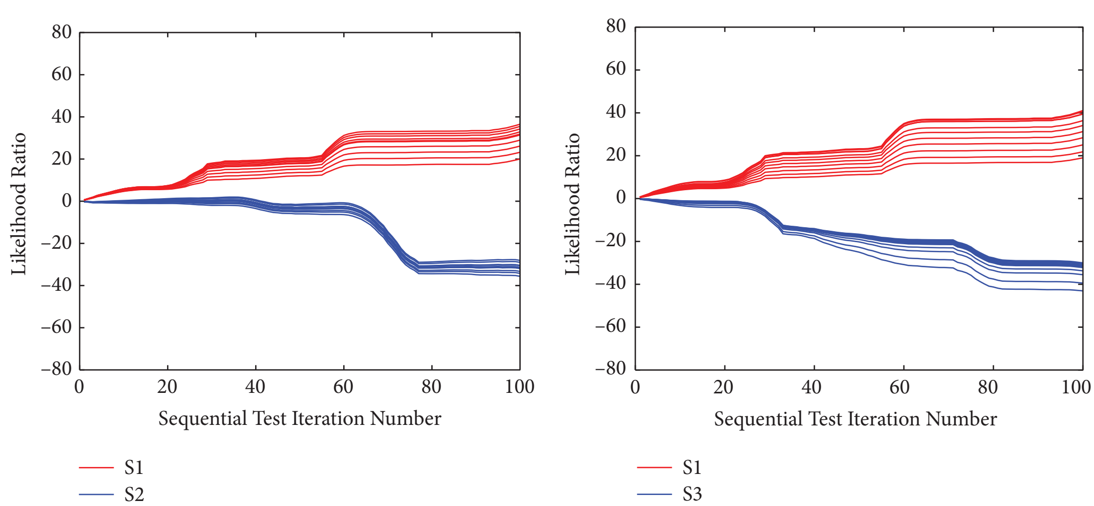

(a) (b)

Figure 11: Continued.

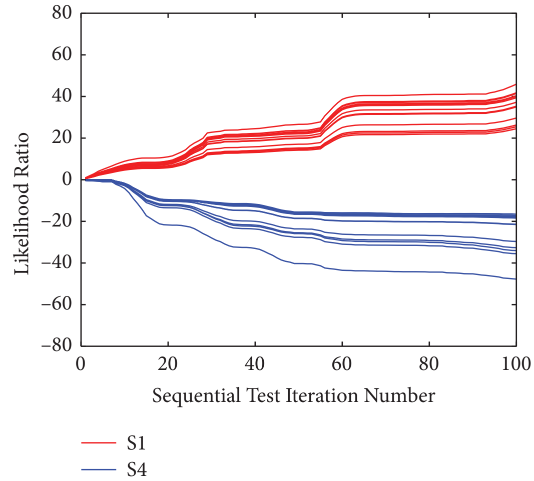

(c)

Figure 11: Sequential probabilistic ratio test results between two samples (a) $s1$ and $s2$; (b) $s1$ and $s3$; and (c) $s1$ and $s4$.

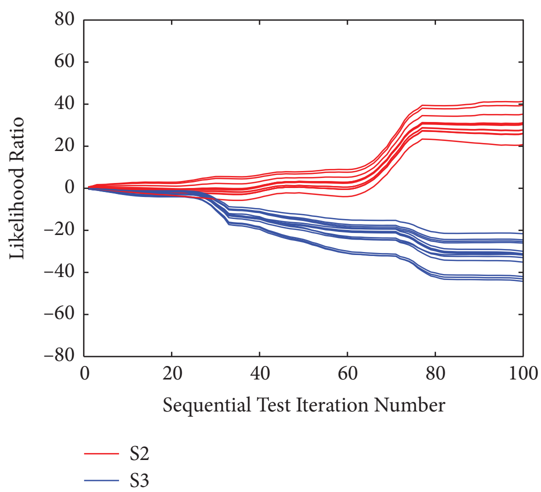

(a)

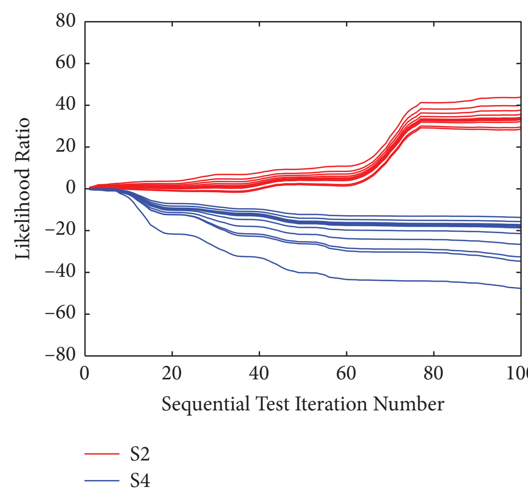

(b)

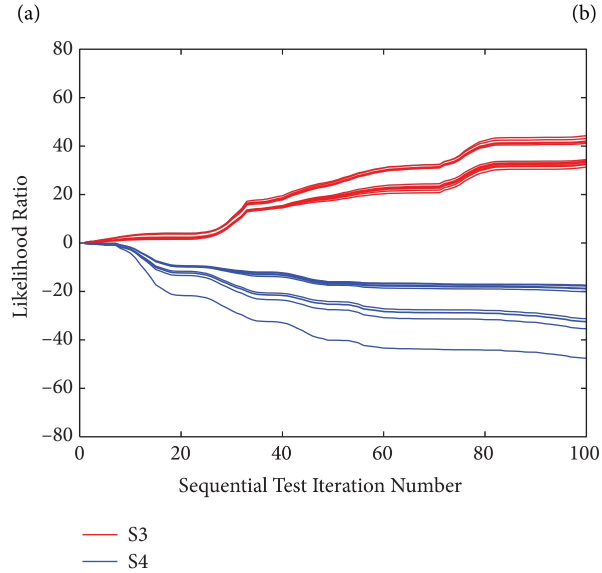

(c)

Figure 12: The sequential probability ratio test between two fatigue damage samples: (a) $S2$ and $S3$, (b) $S2$ and $S4$, and (c) $S3$ and $S4$.

mean value of $S1$ without damage is taken as the parameter μ_0 and the mean value of $S4$ is taken as the parameter μ_1 for testing. When the experimental data under $S1$ state is inputted, the likelihood ratio meets $\Delta < b$, which indicates that the aluminum alloy specimen has no fatigue damage. When the signal under $S4$ sample is input, the likelihood ratio meets $\Delta > a$, which indicates that the aluminum alloy specimen has fatigue damage with 12000 cycles fatigue. Based on the criteria in Figure 11, the input signal is judged to be $S1$ or other three samples.

If it is judged to be $S1$, then the input signal may be $S2$, $S3$, or $S4$. The experimental data under $S2$ are input into SPRT and compared with the data under $S3$ and $S4$. As shown in Figure 12, the proposed sequential probabilistic ratio test algorithm distinguishes the second harmonic signals $S2$, $S3$, and $S4$ under different fatigue damage states. In Figure 12(a), the mean value of signal $S2$ is denoted as parameter μ_0 and the variable value of signal $S3$ is denoted as parameter μ_1. The $S2$ and $S3$ are respectively input into the likelihood ratio formula to test the second harmonic signals. Similarly, the mean value of signal $S2$ is denoted as μ_0 and the mean value of signal $S4$ is denoted as μ_1. The $S2$ and $S4$ are input into the likelihood ratio formula, respectively, for testing. The SPRT results are shown in Figure 12(b). Based on the comparison between $S2$ and $S3$ or $S4$, it is judged the sample is $S2$ or not.

If it is sure the sample is not $S2$, it is judged that the sample is $S3$ or $S4$. The procedure continues to compare $S3$ and $S4$. The variable value of the signal $S3$ is taken as μ_0 and the mean value of signal $S4$ is taken as μ_1. The second harmonic signal under $S3$ and $S4$ are respectively input into the SPRT algorithm. The test results shown in Figure 12(c) are obtained. It is judged to be $S3$ or $S4$ by the criteria as shown in (12)–(14).

Figure 12(a) shows that when the input signals are $S2$, the likelihood ratio satisfies $\Delta < b$. The input signal $S3$ is obtained when the likelihood ratio satisfies $\Delta > a$. It can clearly and effectively distinguish $S2$ with the 4000 cycles fatigue damage from $S3$ for the 8000 cycles fatigue damage. In Figure 12(b), when the input signal is $S2$, the likelihood ratio satisfies $\Delta < b$. When the input signal is $S4$, the likelihood ratio satisfies $\Delta > a$. It is effective to distinguish the second harmonic $S2$ with the 4000 cycles fatigue damage from the second harmonic $S4$ collected under the 12000 cycles fatigue damage. Finally, as shown in Figure 12(c), when the input signal is $S3$, the likelihood ratio meets $\Delta < b$. If the input signal is $S4$, it is obtained that the likelihood ratio satisfies $\Delta > a$. It effectively distinguishes the second harmonic $S3$ collected under the 8,000 cycle fatigue stretching and the second harmonic $S4$ collected under the 12,000 cycles fatigue stretching. Based on the procedure as shown in Figures 11 and 12, the samples are identified.

6. Conclusion

In this paper, the sequential probabilistic ratio test for Lamb wave nonlinear signal analysis is studied. Four groups of second harmonics signals were obtained through the nonlinear Lamb experimental detection platform. The sequential probabilistic ratio test algorithm was proposed to identify and test the four groups of second harmonics signals. The results show that the proposed algorithm distinguishes the second harmonic signals without fatigue damage and those with fatigue damages, and also the second harmonic signals with different fatigue degradation.

Data Availability

The data that support the findings of this study are available from the corresponding author upon reasonable request.

Conflicts of Interest

The authors declare no potential conflicts of interest with respect to the research, authorship, and/or publication of this article.

Acknowledgments

This work was supported by the National Natural Science Foundation of China (grant 51775390).

References

[1] L. M. Hui and M. Liu, "Impact mill RTM fiberglass/E51 epoxy composites void content ultrasonic characteristic parameters," *Journal composite material*, vol. 35, no. 2, pp. 291–297, 2018.

[2] Z. Zhou and S. Liu, "Research, application and development of nonlinear nondestructive testing technology," *Journal of Mechanical Engineering*, vol. 47, no. 8, pp. 2–11, 2011.

[3] Y. Guo, X. Shi, and G. Wang, "Nonlinear ultrasonic testing of micro-nano-scale cracks," *Editorial Office of Optics and Precision Engineer*, vol. 19, no. 1, pp. 132–137, 2011.

[4] B. S. Yan, B. Wu, C. F. He, and J. P. Jiao, "Early fatigue damage of magnesium alloy on-line monitoring by nonlinear ultrasonic," *Advanced Materials Research*, vol. 139-141, pp. 194–197, 2010.

[5] M. Deng, Y. Xiang, and L. Liu, "Time-domain analysis and experimental examination of cumulative second-harmonic generation by primary Lamb wave propagation," *Journal of Applied Physics*, vol. 109, Article ID 113525, 2011.

[6] M. Deng, "A nonlinear ultrasonic Lamb wave method for evaluating surface properties of solid sheets," *Applied Acoustics*, vol. 32, no. 4, pp. 262–269, 2013.

[7] M. F. Müller, J. Y. Kim, J. Qu, and L. J. Jacobs, "Characteristics of second harmonic generation of Lamb waves in nonlinear elastic plates," *Journal of the Acoustical Society of America*, vol. 127, no. 4, pp. 2141–2152, 2010.

[8] Y. Wang, R. Guan, and Y. Lu, "Nonlinear Lamb waves for fatigue damage identification in FRP-reinforced steel plates," *Ultrasonics*, vol. 5, no. 80, pp. 87–95, 2017.

[9] C. Bermes, J. Y. Kim, J. Qu, and L. J. Jacobs, "Nonlinear Lamb waves for the detection of material nonlinearity," *Mechanical Systems and Signal Processing*, vol. 22, no. 3, pp. 638–646, 2008.

[10] D. Dutta, H. Sohn, K. A. Harries, and P. Rizzo, "A nonlinear acoustic technique for crack detection in metallic structures," *Structural Health Monitoring*, vol. 8, no. 3, pp. 251–262, 2009.

[11] C. Pruell, J.-Y. Kim, J. Qu, and L. J. Jacobs, "Evaluation of fatigue damage using nonlinear guided waves," *Smart Materials and Structures*, vol. 18, Article ID 35003, 2009.

[12] F. Martin, “Müller, Jin-Yeon Kim, Jianmin Qu, etal. Characteristics of second harmonic generation of Lamb waves in nonlinear elastic plates,” *Journal of the Acoustical Society of America*, vol. 127, no. 4, pp. 2141–2152, 2010.
[13] A. Wald, *Sequential Analysis*, Wiley, New York, NY, USA, 1947.
[14] N. A. Goodman, R. V. Phaneendra, and M. A. Neifeld, “Adaptive waveform design and sequential hypothesis testing for target recognition with active sensors,” *Journal of Selected Topics in Signal Processing*, vol. 1, no. 1, 2007.
[15] Z. H. Min and L. M. Sun, “A Novel Non-parametric Sequential Probability Ratio Test Method for Structural Condition Assessment,” in *Proceedings of the Health Monitoring of Structural and Biological Systems*, San Diego, CA, USA, April 2010.
[16] H. X. Chen, Y. F. Shang, and K. Sun, “Multiple fault condition recognition of gearbox with sequential hypothesis test,” *Mechanical system and signal processing*, vol. 40, no. 2, pp. 469–482, 2013.
[17] J. L. Rose, *Ultrasonic Guided Waves in Solid media*, Cambridge University Press, Cambridge, UK, 2014.